Monte Carlo calculations in comparison to neutron scattering studies: 1. Linear chains

Klaus Huber, Walther Burchard and Siegfried Bantle*
Institute of Macromolecular Chemistry, University of Freiburg, D-7800 Freiburg, FRG
(Received 9 July 1986; accepted 13 October 1986)

The structures of linear polystyrene chains as well as of generated rotational isomeric state backbone chains are discussed in the light of the worm-like chain model. The global dimensions of these linear chains are represented satisfactorily by the theory of Kratky and Porod, if the system is under θ conditions. The particle scattering factors of backbone chains, consisting of point scatterers, can be described well by the theory of Koyama up to a certain q range. In the crossover region of coiled to rod-like behaviour, significant deviations occur. The particle scattering factors of polystyrene chains are approximated well by the theory of Koyama in the low q range. The range of validity in q is enlarged by introducing an effective chain thickness correction. During the change of solvent from cyclohexane to toluene, the structure of polystyrene chains is modified by two independent effects (i) enhanced long-range interactions due to the excluded volume; (ii) a change in short-range interactions, which modifies the chain stiffness of polystyrene. The second effect may be explained by specific interactions between the benzene rings of styrene and toluene.

(Keywords: rotational isomeric state simulation; stiff linear chains; Koyama theory; scattering functions; SANS)

INTRODUCTION

The rotational isomeric state (r.i.s.) model, developed in the 1960s by Flory[1], has proved to be a powerful method to describe geometric chain behaviour. As a straightforward refinement of the 'equivalent' freely jointed chain model of Kuhn[2] and of the 'persistence' chain model of Kratky and Porod[3], it gives a more detailed picture of polymeric configuration down to the order of magnitude of the monomeric units.

The basis of the r.i.s. approximation is the idea to describe the configuration of a polymeric chain with a Markovian sequence of interdependent rotational isomeric states of skeletal bonds. Under the assumption of three fixed rotational angles and assuming that those states depend only on the preceding angle, each step in the Markovian sequence is determined by the elements $p_{\zeta\eta;i}$ of a 3×3 matrix.

$$\mathbf{P}_i = [p_{\zeta\eta;i}] \tag{1}$$

Here, $p_{\zeta\eta}$ is the *a priori probability* that bond i is in the r.i.s. η if the preceding bond is in state ζ. The row index ζ stands for the r.i.s. state of bond $i-1$ and the column index for bond i.

The matrix $\mathbf{P}_i$ is calculated starting from the *statistical weights* $u_{\zeta\eta;i}$ that bond i is in state η when bond $i-1$ is in state ζ, which are defined as

$$u_{\zeta\eta;i} = \exp(-E_{\zeta\eta;i}/RT) \tag{2}$$

where by definition $E_{\zeta\eta;i}$ is the energy difference of bond i between the initial *trans* state and state η, if bond $i-1$ is in state ζ. All preceding bonds are in their already assigned state and all succeeding bonds in the standard state, which is the *trans* state. $\mathbf{U}_i$ is therefore called the statistical weight matrix

$$\mathbf{U}_i = [u_{\zeta\eta;i}] \tag{3}$$

η and ζ can assume the following three r.i.s. states: *trans* (t), *gauche*$^+$ (g^+) and *gauche*$^-$ (g^-).

At this point, it has to be emphasized that the elements of the matrix $\mathbf{U}_i$ are not probabilities but terms of the three rotational partition functions (statistical weights), each of which is determined by the respective state of its predecessor. It therefore cannot be used directly to simulate a Markov chain.

For infinitely long chains, $\mathbf{U}_i$ is independent of special location along the chain and the index i can be omitted. Similarity transformation[4] of $\mathbf{U}$ then leads to the final matrix $\mathbf{P}$, necessary for the generation of a Markovian chain.

As was pointed out by Jernigan *et al.*[5] for a polymethylene (PM) chain at 140°C the values of $p_{\zeta\eta;i}$ start to deviate significantly from the limiting values only if the location is less than five bonds from the chain ends. This location dependence is of minor consequence for the geometric size[6], even for very low bond numbers. The calculations performed in this paper correspond to 'chain segments' with n_B bonds within an infinitely long chain, and disregard special chain-end effects.

In this paper the Monte Carlo technique is used, on the one hand, to generate a certain number of r.i.s. carbon backbone chains. On the other hand, experimental results have been obtained from small-angle neutron scattering (SANS) measurements on linear polystyrene (PS) in toluene-d_8 and cyclohexane-d_{12}. The chain contour length of these PS molecules are comparable to those of the simulated PM chains.

For an interpretation of both sets of data, the Koyama theory[7], which approximates the particle scattering factor of continuously bonded chains, was applied. This application to the well defined Monte Carlo data gave insight into the advantages and limits of the Koyama theory. With this knowledge, the Koyama theory now could be applied with confidence to the interpretation of the experimental SANS data.

EXPERIMENTAL

Computer simulations

The computer simulations were carried out with a Sperry Univac 1100/81 configuration at the calculation

* Institut Laue–Langevin, Grenoble, France; present address: Sandoz AG, Basel, Switzerland.

0032-3861/87/060863-10$03.00

centre of the University of Freiburg. Programming language was FORTRAN 77. For the characterization of one backbone chain length, at least 1000 different configurations were generated. $\langle S^2\rangle_z$ of a certain chain length could be reproduced within a range of 2%. Only for the longest chain ($n_B=280$), was the inaccuracy somewhat larger. The adequacy of the Monte Carlo simulations at least for $\mathbf{P}_{M1}$ and $\mathbf{P}_{M3}$ in equations (9a) and (9c) is confirmed by comparing the characteristic ratios estimated here with those obtained by statistical mechanical averaging[6].

Polymers

SANS measurements were carried out with six different PS samples in toluene-d_8 at 20°C and in cyclohexane-d_{12} at 35°C. The molecular weight of the samples was $1000 < M_w < 25\,000$. The origin of the samples as well as the dilute-solution behaviour detected by light and neutron scattering measurements was reported in ref. 8.

Small-angle neutron scattering

Measurements were performed at the Institut Max von Laue–Paul Langevin (ILL), Grenoble, France. All experiments were carried out with the D-17 instrument, where a 64 × 64 cell matrix assembly[9] is used for detecting the scattering intensity. The wavelength of the neutrons was 1.0 nm. To get information about the scattering behaviour over a relatively large q range, two different detector alignments were used. In the first alignment the detector was positioned at a distance to the sample of 2.81 m with an angle of 0° to the primary beam. This provided a q range of $0<q<1\,\text{nm}^{-1}$. In the second alignment, a distance of 1.40 m was chosen and the detector was swung out for 20°; this yielded a q range of $0.9\,\text{nm}^{-1}<q<3.6\,\text{nm}^{-1}$. The solvents cyclohexane-d_{12} and toluene-d_8 were used without further purification (98% D; from Merck Sharp and Dohme, Canada).

Evaluation of small-angle neutron scattering data

Evaluation of the scattering data was performed at the ILL according to the following procedure[10].

Prior to each measurement of the scattering intensity of a sample, the transmission T_s of this sample was determined. T_s is the ratio of the intensity impinging on the detector with and without the sample in the cell holder. Together with the intensity of the samples i_s, the following intensities were measured: i_{EC} (empty cell), i_{H_2O} (standard H_2O) and i_{SB} (sample background corresponding to the respective solvent). Assuming isotropic scattering behaviour of all intensities, radial averaging was performed. Using these q-dependent intensities, the effective scattering cross section per unit volume of the sample $(d\Sigma/d\Omega)_S$ was calculated according to the following equation:

$$\left(\frac{d\Sigma}{d\Omega}\right)=\frac{[i_s(q)-(T_s/T_{SB})i_{SB}(q)]d_{H_2O}T_{H_2O}}{[i_{H_2O}(q)-(T_{H_2O}/T_{EC})i_{EC}(q)]d_sT_s}\left(\frac{d\Sigma}{d\Omega}\right)_{H_2O} \quad (4)$$

with d_{H_2O} and d_S the thickness of the standard and sample respectively and $(d\Sigma/d\Omega)_{H_2O}$ the known effective scattering cross section per unit volume of the standard.

Equation (4) still contains the incoherent part of the scattering cross section. To get the exact $P(q)$, M_w and $\langle S^2\rangle_z$, a correction for the incoherent scattering intensity is necessary. Under the assumption that the incoherent scattering from carbon and deuterium atoms is equal both in sample and solvent, the incoherent scattering cross section of the sample is due to the H-atom content of the polymer alone and may be estimated according to the following relationship:

$$\left(\frac{d\Sigma}{d\Omega}\right)_S^{inc}=c\left(\frac{\sigma^{inc}}{4\pi}n_H\frac{N_A}{M_2}\right) \quad (5)$$

with c the concentration of polymer (in g cm^{-3}), N_A the Avogadro number σ^{inc} the incoherent scattering cross section of the H atom and n_H the number of hydrogen atoms of the monomeric unit styrene with molecular weight M_2. For σ^{inc} a value of $\sigma^{inc}=(105\pm7)\times10^{-24}\,\text{cm}^2$ was used, which was determined by Raviseau[11] with polystyrene-h in CS_2.

To get to the final value of $(Kc/(d\Sigma/d\Omega))^{coh}$ with the dimensions mol g^{-1} the contrast factor K was calculated according to

$$K=(L_2^{coh}-L_1^{coh}\rho_1\bar{v}_2) \quad (6)$$

where ρ_1 is the density of the solvent, $\bar{v}_2$ the partial specific volume of the polymer and

$$L_K^{coh}=N_A\sum^{n_A}b_\alpha/M_k \quad (7)$$

$\sum^{n_A}b_\alpha$ is the sum over the scattering lengths of all n_A atoms of solvent ($k=1$) and monomer ($k=2$). *Table 1* contains the values for $\bar{v}_2$ and ρ_1. The relevant scattering lengths b_α are listed in *Table 2*.

MONTE CARLO CALCULATIONS

The same parameters were used for the PM chain as chosen by Kajiwara *et al.*[12]: The backbone C–C bond of length 0.153 nm was allowed to occur in three fixed rotational angles $\chi=0°$ (t), $+120°$ (g^+) and $-120°$ (g^-); the angle between two neighbouring C–C bonds was taken to be 112°. The statistical weight matrix $\mathbf{U}$ is

$$\mathbf{U}=\begin{pmatrix}1 & \sigma & \sigma\\ 1 & \sigma\psi & \sigma\omega\\ 1 & \sigma\omega & \sigma\psi\end{pmatrix} \quad (8)$$

Table 1 Scattering length and incoherent scattering cross section of H, D and C nuclei

Atom	$b_\alpha(10^{-12}\,\text{cm})^a$	$\sigma^{icoh}(10^{-24}\,\text{cm}^2)^b$
H	−0.374	79.7 105.0 ± 7^c
D	0.667	7.2
C	0.665	0.01

[a] Ref. 14
[b] Ref. 31
[c] Ref. 11, σ^{icoh} of polystyrene-h in CS_2

Table 2 Partial specific volume $\bar{v}_2$ of the polymer and density ρ_1 of the deuterated solvent

Solvent	$\rho_1(\text{g cm}^{-3})$	$\bar{v}_2(\text{cm}^3\,\text{g}^{-1})$
Cyclohexane-d[a]	0.909	0.926
Toluene-d	0.94	0.92

[a] Ref. 29

with $\sigma = 0.54$, $\omega = 0.088$ and $\psi = 1$. These values result from[4] $E_\sigma = 500\,\text{cal mol}^{-1}$, which is the energy of any *gauche* state relative to a *trans* state, and $E_\omega = 2000\,\text{cal mol}^{-1}$, which is the energy of a pair of *gauche* states with different signs in excess of the energy of $2E_\sigma$. The energy of two neighbouring *gauche* bonds of the same sign E_ψ is assumed to be approximately equal to $2E_\sigma$. The chosen differences correspond to a PM chain at 140°C which is a θ state of this polymer.

When the above-mentioned values for $u_{\zeta\eta}$ the matrix **P** is given as:

$$\mathbf{P}_{M1} = \begin{pmatrix} 0.321 & 0.138 & 0.138 \\ 0.138 & 0.059 & 0.0052 \\ 0.138 & 0.0052 & 0.059 \end{pmatrix} \quad (9a)$$

To generate chains of different rigidity, we carried out the same calculations with two further sets of energies for E_σ, E_ω and E_ψ. The first set significantly increases the frequency of *trans* states. Assuming $E_\sigma = 800\,\text{cal mol}^{-1}$, $E_\omega = \infty$ and $E_\psi = 0$, the following *a priori* probabilities are obtained:

$$\mathbf{P}_{M2} = \begin{pmatrix} 0.415 & 0.127 & 0.127 \\ 0.127 & 0.039 & 0 \\ 0.127 & 0 & 0.039 \end{pmatrix} \quad (9b)$$

For the second set, mutual independence of rotational potentials was assumed, which is equivalent to $E_\sigma = 500\,\text{cal mol}^{-1}$, $E_\psi = 0$ and $E_\omega = 0$. This leads for the *a priori* probabilities to:

$$\mathbf{P}_{M3} = \begin{pmatrix} 0.16 & 0.087 & 0.087 \\ 0.16 & 0.087 & 0.087 \\ 0.16 & 0.087 & 0.087 \end{pmatrix} \quad (9c)$$

Application of a random number generator to the respective rows of this matrix yields the Markov chain of succeeding r.i.s. states. This Markov chain determines the sequence of bond transformations, which results in n_B 'transformed bonds'. The linear combination of these bonds yields the polymer chain in its final conformation. Details are given in the Appendix.

For each simulation of a chain with n_B bonds at least 1000 different conformations were produced. During the simulation, the program carried out the following procedures, where $n_A = n_B + 1$ is the number of skeletal atoms:

(i) After determination of a Markov chain consisting of n_B r.i.s. states, attached to bond 1 to $n_B - 1$, the coordinates of the bond vectors $r_j - r_{j-1}$ with $1 \leqslant j \leqslant n_A$ were calculated.

(ii) With these bond vectors, all intramolecular distances $r_j - r_i$ were calculated and stored in histograms consisting of 100 grids each. The number of histograms is $n_B - 2$. The histogram in which a distance $r_j - r_i$ was stored dependend only on its number of segments $n = j - 1$. This procedure presupposed independence of $r_n = r_j - r_i$ of the location along the chain.

(iii) From these histograms, the following conformational quantities were obtained: $\langle 1/r_n \rangle$, $\langle r_n^2 \rangle$, $\langle r_n \rangle$ and $\langle \sin(r_n q)/(r_n q) \rangle$. The angular brackets denote mean values over all calculated configurations and q is the scattering vector in nanometres.

(iv) According to the relationships below the mean-square end-to-end distance $\langle R^2 \rangle$, the mean-square radius of gyration $\langle S^2 \rangle$, the hydrodynamic radius R_h and the particle scattering factor $P(q)$ were then calculated:

$$\langle R^2 \rangle = \langle r_{n\beta}^2 \rangle \quad (10)$$

$$\langle S^2 \rangle = 1/n_A^2 \left(\sum_{n=1}^{n_A} \langle r_n^2 \rangle (n_A - n) \right) \quad (11)$$

$$1/R_h = 1/n_A^2 \left(\sum_{n=1}^{n_B} 2\langle 1/r_n \rangle (n_A - n) \right) \quad (12)$$

$$P(q) = 1/n_A^2 \left(\sum_{n=1}^{n_A} 2\langle \sin(r_n q)/(r_n q) \rangle (n_A - n) + n_A \right) \quad (13)$$

(v) From a further histogram, consisting of 60 grid points with step length Δr, the probability $g(i\Delta r)$ of finding from a randomly selected skeletal atom in a distance interval $(i-1)\Delta r < r_n < i\Delta r$ another skeletal atom of the same chain was calculated:

$$g(i\Delta r) = h(i\Delta r) / \left(\Delta r \sum_{i=1}^{60} h(i\Delta r) \right) \quad (14)$$

where $h(i\Delta r)$ is the number of distances r_n occurring within the interval $(i-1)\Delta r < r_n < i\Delta r$, and $g(i\Delta r)$ is proportional to the well known density–density correlation function $\langle \rho(0)\, \rho(r) \rangle$.

GLOBAL DIMENSIONS

To describe the coil dimensions of linear polymers, Kratky and Porod[3] used the model of a continuously bonded stiff chain. The finite rigidity in this model is characterized by the persistence length, which is half the Kuhn length l_K. The equation for the end-to-end distance reads

$$\langle R^2 \rangle = l_K^2 n_K - l_K^2/2 + l_K^2 e^{-2n_K} \quad (15)$$

where n_K is the number of Kuhn segments per chain. The corresponding mean-square radius of gyration for the same model chain was calculated by Benoit and Doty[15]:

$$\langle S^2 \rangle = l_K^2/6 + l_K^2/4(1/n_K - 1) - (l_K^2/8n_K^2)(1 - e^{-n_K}) \quad (16)$$

To describe the molecular-weight dependence of $\langle S^2 \rangle$ the two parameters l_K and m_L are needed where the latter is the mass per unit length; it is related to the contour length $L$and the molecular weight M according to

$$L = M/m_L \quad (17a)$$

The two parameters l_K and m_L can be obtained either from a direct fit to the experimental data, using equation (16), or from a plot of C_s ($\equiv \langle S^2 \rangle / M_w$) *versus* log M_w using the relationships[17]

$$\lim_{M \to \infty} C_s = C_{s\infty} = l_K/6m_L \quad (18)$$

and

$$M_{1/2} = 3.54 m_L l_K/2 \quad (19)$$

with $M_{1/2}$ the molecular weight at which $C_s = C_{s\infty}/2$. C_s is a characteristic ratio for chains of finite length which is based on the radius of gyration $\langle S^2 \rangle^{1/2}$.

Figure 1 represents the experimental data of $\langle S^2 \rangle$ for PS in cyclohexane-d_{12} (ref. 8), which can be well described by equation (16) if the values $l_K = 2$ nm and $m_L = 430$ (g mol^{-1} nm^{-1}) (*Table 4*) are used. These results

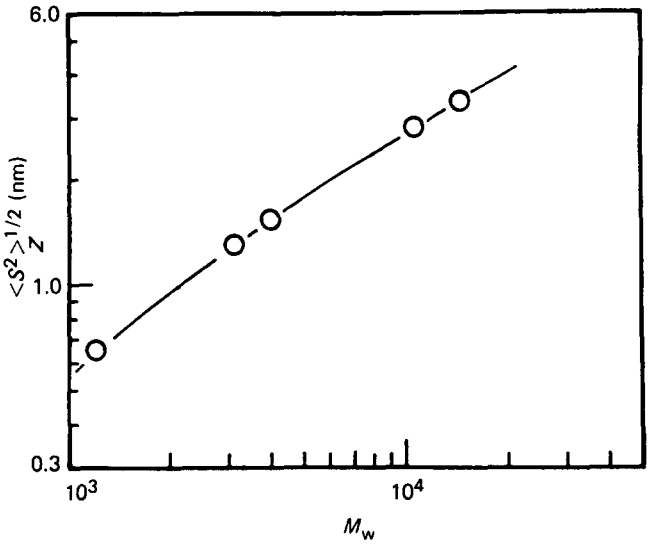

Figure 1 Plot of $\langle S^2\rangle_z^{1/2}$ from SANS experiments in cyclohexane-d_{12} at 35°C. The curve is calculated according to equation (22)

Table 3 Radius of gyration $\langle S^2\rangle^{1/2}$, end-to-end distance $\langle R^2\rangle^{1/2}$ and hydrodynamic radius R_h from Monte Carlo simulations

Modification 1			
n_B	$\langle S^2\rangle^{1/2}$(nm)	$\langle R^2\rangle^{1/2}$(nm)	R_h(nm)
10	0.335	0.949	0.352
24	0.632	1.749	0.522
30	0.741	2.051	0.585
62	1.164	3.058	0.843
80	1.354	3.496	0.960
205	2.273	5.616	1.553
280	2.721	6.861	1.836
Modification2			
n_B	$\langle S^2\rangle^{1/2}$(nm)	$\langle R^2\rangle^{1/2}$(nm)	R_h(nm)
10	0.349	1.011	0.358
24	0.677	1.923	0.540
30	0.790	2.209	0.604
62	1.274	3.387	0.889
80	1.492	3.912	1.020
205	2.552	6.437	1.686
280	3.032	7.648	1.991
Modification 3			
n_B	$\langle S^2\rangle^{1/2}$(nm)	$\langle R^2\rangle^{1/2}$(nm)	R_h(nm)
10	0.306	0.809	0.330
24	0.520	1.352	0.455
30	0.587	1.500	0.496
62	0.888	2.247	0.683
80	1.012	2.526	0.764
205	1.611	4.035	1.170
280	1.973	4.873	1.420

are in agreement with the findings of Ballard *et al.*[18] and Norisuye *et al.*[17], and complete the picture.

This fitting procedure is repeated then for the three simulated r.i.s. chain systems. The overall dimensions are collected in *Table 3*. Here $n_L(\equiv n_K/L)$ is used instead of m_L with

$$L = n_A/n_L \qquad (17b)$$

Furthermore, the parameters $C_s = \langle S^2\rangle/n_A$ and $n_{1/2}$ instead of $\langle S^2\rangle/M_w$ and $M_{1/2}$ are used. Values for the parameters l_K and n_L are estimated with equations (18) and (19) from a plot of $\langle S^2\rangle/n_A$ *versus* $\log n_A$ (*Figure 2*). The results of this estimation are given in *Table 4*. In all cases equation (16) with the parameters of *Table 4* provide a good description of the data, which are shown in *Figure 3* in double logarithmic plot.

It is worth mentioning that with increasing $C_{s\infty}$, the number of backbone atoms per unit length n_L is increased. This can be discussed as follows. In principle, two different possibilities exist for predicting theoretical values for $n_L = n_A/L$ The first is based on the end-to-end distance of the chain in the *all-trans conformation:*

$$L^{(1)} = n_B 0.153 \cos 34° \quad \text{(nm)} \qquad (20a)$$

whereas in the second, the contour length goes along each chemical bond:

$$L^{(2)} = n_B 0.153 \quad \text{(nm)} \qquad (20b)$$

For a carbon–carbon chain, equation (20a) yields $n_L^{(1)} = 7.88$ nm and equation (20b) $n_L = 6.54$ nm.

Within the spread of error due to the graphical determination of $C_{s\infty}$ and $n_{1/2}$, the n_L values in *Table 4* indicate an increasing influence of the zig-zag structure on

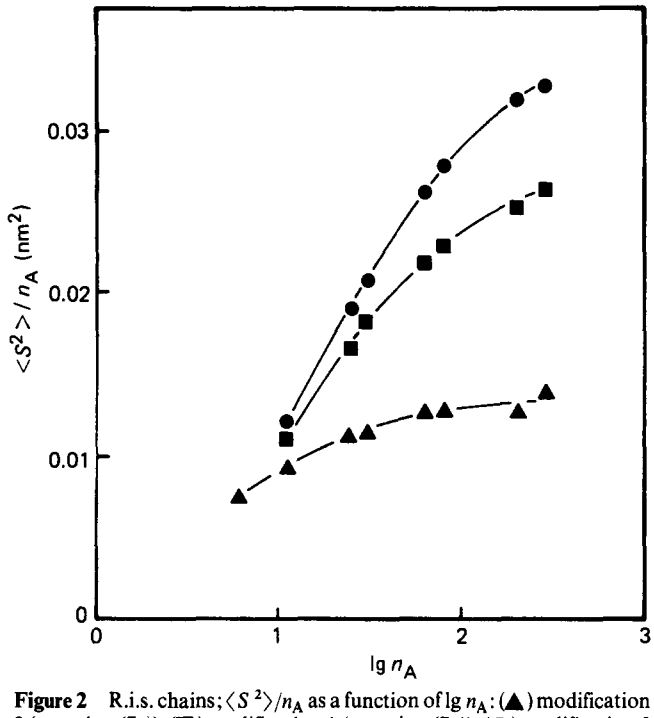

Figure 2 R.i.s. chains; $\langle S^2\rangle/n_A$ as a function of lg n_A: (▲) modification 3 (equation (7c)), (■) modification 1 (equation (7a)), (●) modification 2 (equation (7b))

Table 4 Values of $n_{1/2}$ and $C_{s\infty}$ from *Figure 2* and the resulting parameters n_L and l_K of the r.i.s. chains together with the parameters m_L and l_K for PS

Chain parameters of r.i.s. chains				
Modification	$n_{1/2}$(nm^{-1})	$C_{s\infty}$(nm^2)	n_L(nm^{-1}	l_K(nm)
III	4.8	0.0133	5.86	0.46
I	15.5	0.0269	7.37	1.19
II	21.4	0.0353	7.55	1.60
Chain parameters of PS				
Solvent		m_L (g mol^{-1} nm^{-1})		l_K(nm)
PS in cyclohexane		430		2.0
PS in toluene		450		2.9

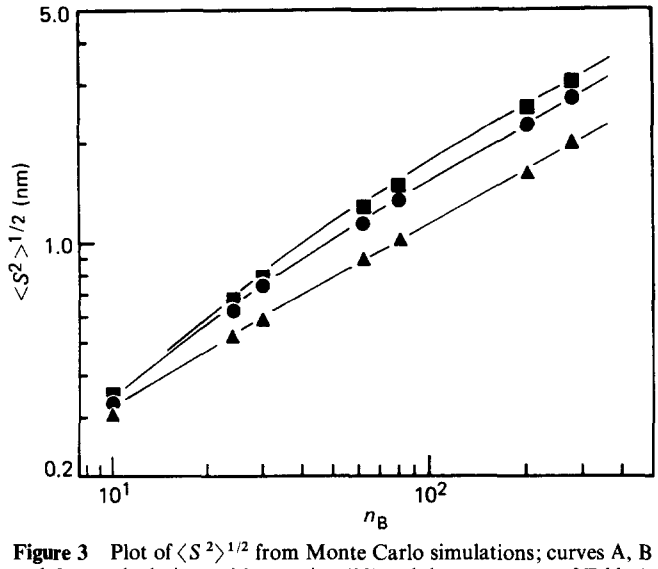

Figure 3 Plot of $\langle S^2\rangle^{1/2}$ from Monte Carlo simulations; curves A, B and C are calculations with equation (22) and the parameters of *Table 4*: symbols as in *Figure 2*

the contour length of the model chain if chain stiffness decreases. This implies a decrease of n_L or m_L. In the case of PS, the experimental $m_L = 430$ (g mol^{-1} nm^{-1}) yields a contour length which lies around the end-to-end distance of the PS chain in the all-*trans* conformation, where equation (20a) holds.

The ρ ratio

For a further characterization of the r.i.s. chains, the dimensionless parameter ρ is introduced:

$$\rho = \langle S^2\rangle^{1/2}/R_h \qquad (21)$$

Using the data from *Table 3*, a certain dependence of ρ on the chain length is observed, which is shown in *Figure 4*. For all three modifications of **P**, ρ depends linearly on $n_B^{-1/2}$, and an extrapolation towards infinite chain length provides accurate limiting values of ρ_∞ which are $\rho_\infty = 1.42$ ($\mathbf{P}_{M3}$), 1.50 ($\mathbf{P}_{M1}$) and 1.55 ($\mathbf{P}_{M2}$). According to Kirkwood and Riseman[19], R_h is defined by the equation:

$$1/R_h = \frac{1}{n_K a_h} + \frac{2(6/\pi)^{1/2}}{l_K n_K^2} \sum_{n=1}^{n_K-1} (n_K - n) n^{-1/2} \qquad (22)$$

with a_h the effective hydrodynamic radius of a Kuhn segment. The first term in (22) (free draining term) is proportional to n_A^{-1}; the second (non-draining) term becomes proportional to $n_A^{-1/2}$ if n_A is large. Thus, with increasing n_A, the first term can be omitted and the free draining term should be a good approximation to R_h.

The procedure of calculating values for R_h from simulated chains (equation (14)) neglects the free draining term and we confine ourselves to the extrapolated ρ_∞ value. As can be seen from *Figure 4*, this value increases slightly with increasing chain stiffness. This unexpected behaviour confirms the findings of Kajiwara *et al.*[12,34], who performed similar Monte Carlo simulations for several chemically different backbone chains.

The square root of the second moment of the interparticle distance distribution $\langle S^2\rangle^{1/2}$ as well as the -1 moment $1/R_h$ are proportional to $M^{1/2}$. Evidently the more extended Kuhn length has a different influence on the limiting geometric dimensions than on the hydrodynamic ones. As long as only the centres of mass of the individual Kuhn segments are considered, Gaussian chain statistics is strictly valid and the Kirkwood–Riseman theory can be applied. For r.i.s. chains (and real polymers) with an appreciable extension of the segments, Gaussian statistics does not hold for all distances. However, as far as the mean-square radius of gyration in the limit of long chains (i.e. $n_K \gg 1$) is concerned, Gaussian statistics holds. The situation is different for the hydrodynamic radius. Here, the actual non-Gaussian distance distribution for short distances contributes significantly to R_h. This additional contribution occurs in the actual r.i.s. calculation, since this is based on the *monomer* centres and not on those of the Kuhn segments. As a consequence of this, the ρ parameter becomes sensitive to the microstructure as soon as the Gaussian chain model is left.

All three limiting values of ρ lie around 1.5 in agreement with the prediction of Kirkwood and Riseman[19] and therefore are well above the experimentally determined ρ values[20,21].

STRUCTURE AND FACTORS OF r.i.s. CHAINS

As far as we know, there exist only two papers dealing with intra particule scattering behaviour of simulated chains. Zierenberg *et al.*[22] determined the structure factor of a PM chain with 1000 C–C bonds and compared it with the scattering curve predicted by theory, where the terms of the Nagai series[23] expansion was used to calculate $\langle \sin(qr_{ij})/(qr_{ij})\rangle$. In another paper, Kajiwara and Burchard[12] compared the scattering curves of several chemically different r.i.s. backbone chains.

In the present paper, the influence of chain length and chain stiffness on the scattering curves of C–C backbone chains is investigated in more detail. As already mentioned, the influence of chain stiffness was achieved by modifying the statistical weights of rotational isomeric states.

The simulated scattering curves were then interpreted in terms of the Koyama theory[7]. According to this theory,

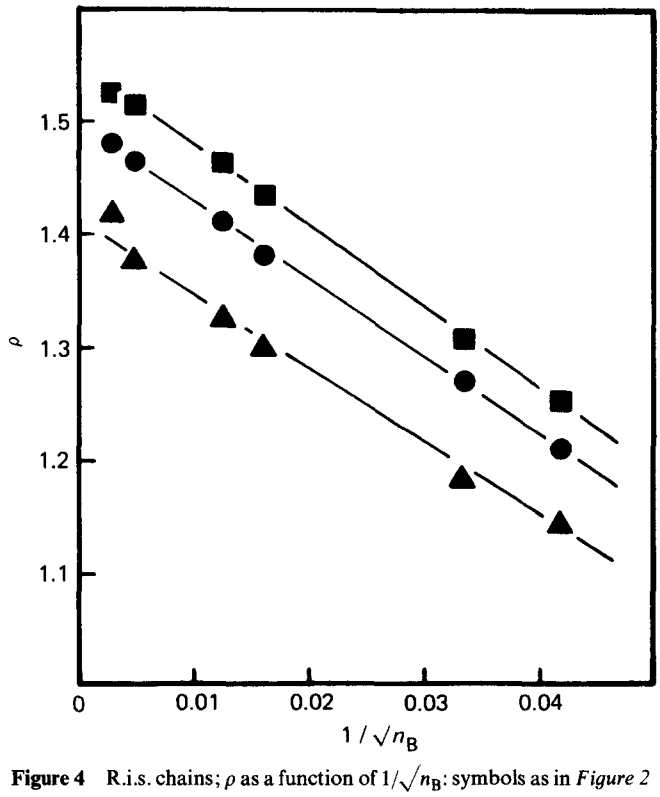

Figure 4 R.i.s. chains; ρ as a function of $1/\sqrt{n_B}$: symbols as in *Figure 2*

the particle scattering factor for monodisperse worm-like chains is given by the equation:

$$P_K(q)=\frac{1}{L^2}\int_0^R (L-x)\exp[-\tfrac{2}{3}q^2 x f(x)]\frac{\sin(qx)g(x)}{qxg(x)}dx \quad (23)$$

The variable x represents the contour length of a part of the chain and $g(x)$ and $f(x)$ are functions of x which are not reproduced here. As for the global dimensions, the two parameters n_L (m_L) and l_K are needed, which are given in *Table 4*.

In *Figure 5*, a comparison is made with the scattering curves of the longest generated chains in both the most flexible and the stiffest case. The scattering curves are represented as Kratky plots, which for the Gaussian chain model eventually approaches a plateau[24]. For the worm-like chain model, this plateau should show a crossover to a linearly increasing part[7,26], i.e. $P(q)q^2 \sim q$, which is typical for rigid rods. The transition q_T is correlated with the persistence length according to[7,25]

$$q_T = 3.82/l_K \quad (24)$$

In contrast to the simple arguments given by Porod[25], the Koyama theory predicts a smooth transition from Gaussian to rod-like behaviour. The curves, which were calculated with the Koyama theory, give a very good approximation of the r.i.s. curves up to a certain q range, but show deviations for q near the crossover region. This q range is shifted towards larger values if the stiffness is decreased. These deviations result from the fact that Koyama spliced together the two analytically exact solutions for the Gaussian and rod-like behaviour, i.e. for small and very large q values respectively. This semiempirical procedure cannot make accurate predictions for the crossover region of intermediate q values.

The molecular-weight dependence of the scattering curve is demonstrated in *Figure 6* for three different chain lengths of PM. In addition, the figure contains the particle scattering factors of the two limiting cases, i.e. (i) the Gaussian coil (curve *b*) for which $\lim_{u\to\infty} P(u)u = 0$ and (ii) the rigid rod (curve A)[27] with $\lim_{u\to\infty} P(u)u = (\pi/2\sqrt{3})$[26]. The scattering curve C shows an approach of the r.i.s. chain with $n_B = 205$ by the Koyama theory.

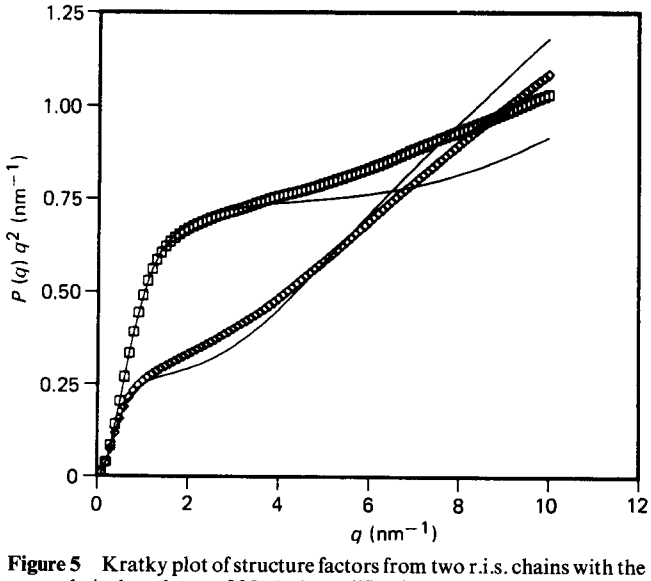

Figure 5 Kratky plot of structure factors from two r.i.s. chains with the same chain length $n_B = 205$: (◇) modification 2 (equation (7b)), (□) modification 3 (equation (7c))

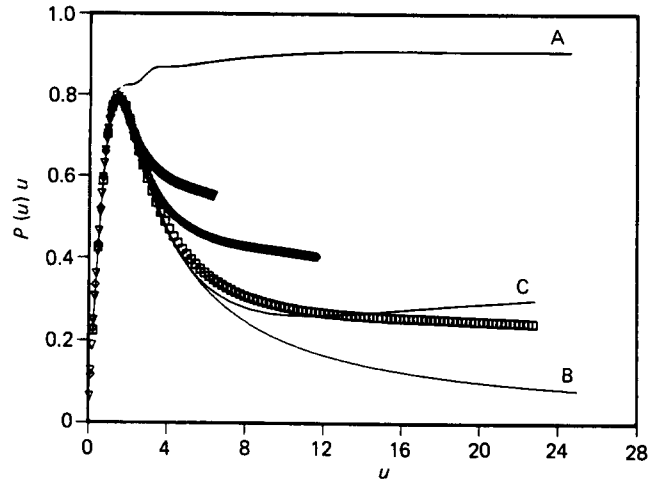

Figure 6 Normalized Holtzer plots; all chains were generated with equation (7a): (▽) $n_B = 24$, (◇) $n_B = 62$, (□) $n_B = 205$, (A) rigid rod[27], (B) Gaussian coil[24], (C) Koyama fit[7] for the r.i.s. chain with $n_B = 205$

Table 5 Values of $\langle S^2\rangle^{1/2}$ of linear PS chains determined by SANS experiments at $T = 35°C$

Probe	M_w	Toluene $\langle S^2\rangle_z^{1/2}$ (nm)	Cyclohexane $\langle S^2\rangle_z^{1/2}$(nm)
TSK-11	10700	3.33	2.76 2.71[a]
PCC-4	4000	1.70	1.53
PS-3	3100	1.39	1.28
PS-1	2100	0.660	0.654

[a] SANS experiment at 38°C

The normalized Holtzer plot, i.e. $P(u)u$ *versus* u, was used. In such a plot, the difference between a rod and a more flexible chain becomes especially clear by the occurrence of a maximum before a typical rod-like plateau is reached. The scattering behaviour of worm-like chains is in between the two limiting curves (A and B in *Figure 5*). Both a maximum and a finite plateau value occur, if the Holtzer plot is used. As pointed out by Schmidt *et al.*[28], the ratio of the maximum height to the asymptote height can be correlated to l_K, whereas the asymptote height $[P(q)q]_p$ is a function of the contour length and therefore of m_L:

$$[P(q)q]_p = \pi/L = \pi m_L/M_w \quad (25)$$

In the case of r.i.s. chains it is difficult to perform an analysis of the structure factor via equations (24) and (25) because the Kuhn length is relatively small and the q range of interest therefore high. At such high q values, $P(q)$ is already influenced by the microstructure and thickness of the chain.

PARTICLE SCATTERING FACTORS OF POLYSTYRENE CHAINS IN CYCLOHEXANE-d_{12}

We performed neutron scattering experiments with four different samples in cyclohexane-d_{12} at 35°C. *Table 5* is a collection of the samples used for the experiments in cyclohexane-d_{12} and toluene-d_8. According to Strazielle

and Benoit[29], the θ point for PS in cyclohexane-d_{12} should lie arround 40°C, which is 5°C higher than our measuring temperature. However, no significant concentration dependence of the particle scattering factor is recognizable, as can be realized from *Figure 7*, which contains Holtzer plots of the sample PCC-4 at two different concentrations. For this reason, the SANS structure factors at finite concentration can be used to interpret the scattering behaviour of short PS chains at infinite dilution.

To fit the SANS curves of PS in cyclohexane-d_{12} according to the theory of Koyama, we used the same set of parameters as for the description of the overall coil dimensions (*Table 4*). Obviously, the original Koyama theory can describe the scattering behaviour of the sample PCC-4 only for $q < 1.5\ \text{nm}^{-1}$ (curve A of *Figure 8*). The fit is improved if a thickness correction $PQ(q)$ is introduced:

$$P(q) = P_K(q)PQ(q) = P_K(q)\, e^{-(d^2q^2/2)} \qquad (26)$$

Curve B in *Figure 8* represents the thus modified Koyama theory with $d = 0.2$ nm and curve C that with $d = 0.26$ nm, which provides the best overall fit. The parameter d has to be regarded as an 'effective thickness', taking into account all influences of the microstructure. An effective cross section between $0.2 < d < 0.3$ nm for PS is certainly reasonable. Nevertheless, we wish to emphasize that this value is only of qualitative relevance. For $q > 2\ \text{nm}^{-1}$, the scattering intensity is getting very small and the amount of incoherent scattering lies around 20–40%. After $P(q)$ has been corrected for this incoherent scattering, the inaccuracy of the experimental structure factors with 5–10% becomes relatively high.

Figure 9a and *9b* show a comparison of the Koyama theory to the SANS curve of TSK-100 and to the particle scattering factor of the generated PM chain with $n_B = 205$ respectively. The PM chain and the TSK-100 sample have about the same number of backbone atoms. The scattering curves are represented as Kratky plots. In both *Figures 9a* and *9b*, the bare Koyama fit corresponds to curve A. Whereas in the case of PS the theoretical curve

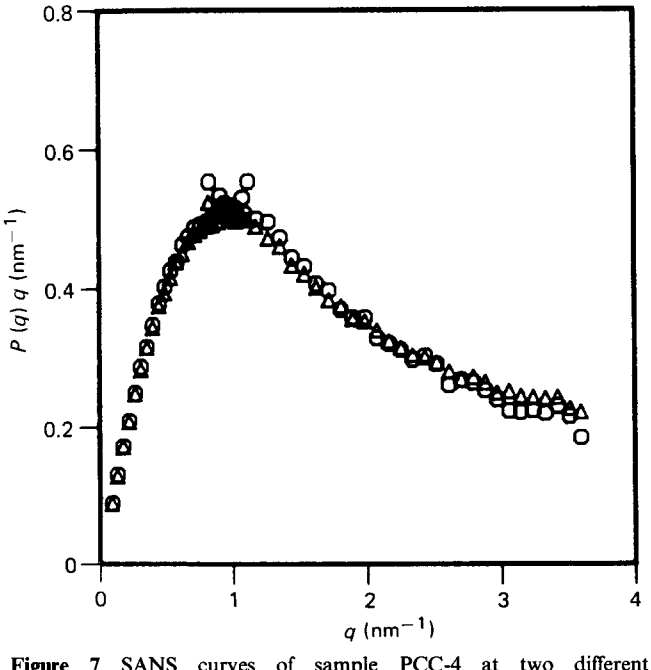

Figure 7 SANS curves of sample PCC-4 at two different concentrations in cyclohexane-d_{12} at 35°C (○), $c = 0.0136\ \text{g cm}^{-3}$, (△) $c = 0.0495\ \text{g cm}^{-3}$

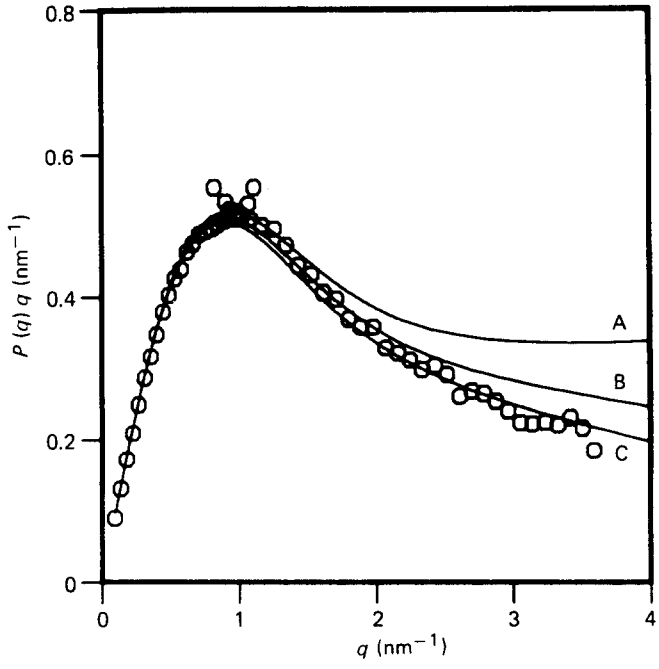

Figure 8 PCC-4 in cyclohexane-d_{12} at $c = 0.0136\ \text{g cm}^{-3}$ and $T = 35$°C; approximations with equation (32): (A) $d = 0$ nm, (B) $d = 0.2$ nm, (C) $d = 0.26$ nm

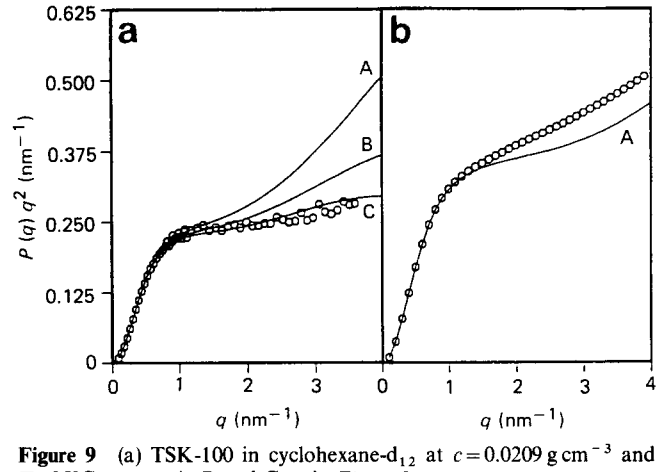

Figure 9 (a) TSK-100 in cyclohexane-d_{12} at $c = 0.0209\ \text{g cm}^{-3}$ and $T = 35$°C: curves A, B and C as in *Figure 8*.
(b) R.i.s. chain with $n_B = 205$, generated according to equation (7a): curve A is an approximation with the theory of Koyama[7]

(A) starts to deviate towards larger values if $q > 1.5\ \text{nm}^{-1}$, the deviation for the PM chain turns in the opposite direction. Only for the PS polymer is a satisfactory description of the scattering curve along the whole q range possible, if a convenient thickness parameter $d = 0.26$ nm is used (curve C). As is immediately understandable, such a thickness correction does not improve the fit for the PM chain, but on the contrary makes it even worse.

Figure 9b demonstrates that the Koyama theory is not a good approximation for the scattering curve in the transition region around q_T. The good fit of the actual PS curve results from the specific hydrogen pattern which brings the scattering curve down to lower values.

THE INFLUENCE OF SOLVENT ON THE PARTICLE SCATTERING FACTOR

Figure 10 represents scattering experiments, similar to those of *Figure 7*, but now performed in the good solvent

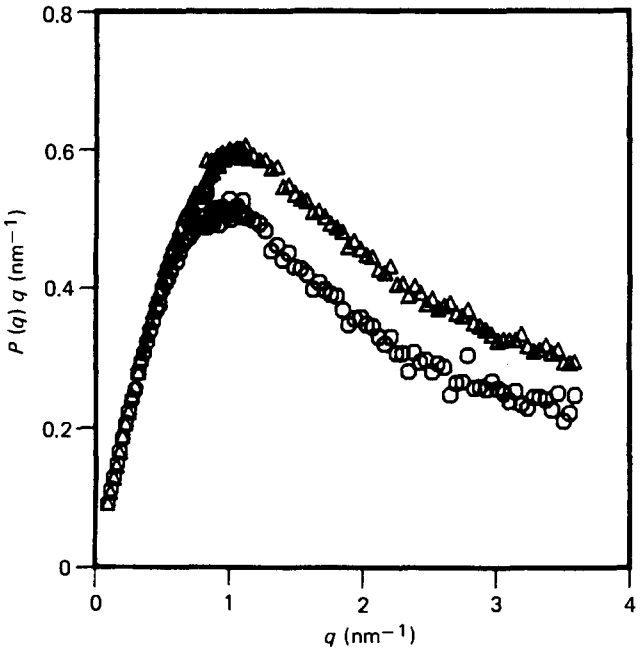

Figure 10 SANS curves of sample PCC-4 at two different concentrations in toluene-d_8 at 20°C: (○) $c = 0.0131\,g\,cm^{-3}$, (△) $c = 0.0492\,g\,cm^{-3}$

toluene-d_8. Clearly, the scattering curves in toluene-d_8 are significantly concentration-dependent and this concentration-dependence changes with q. An appropriate extrapolation of the SANS curves towards $c = 0$ is difficult and does not appear feasible for the moment.

To get still some information from the SANS curves in toluene-d_8, we determined the maximum heights $[P(q)q]_{max}$ in the Holtzer plots; these heights can be determined easily and still lie within the q range in which the Koyama theory with $d = 0$ nm provides a good description of the experimental data. *Figure 11* shows a plot of these maxima *versus* concentration for three different samples, in both cyclohexane-d_{12} and toluene-d_8. In addition, on the ordinate the maximum height according to an approach with the theory of Koyama for PS in cyclohexane is plotted, using $l_K = 2$ nm, $m_L = 430\,g\,nm^{-1}\,mol^{-1}$ and $d = 0.2$ nm. In all three cases, these values give a good description of the infinite-dilution behaviour for the cyclohexane-d_{12} data, but are not able to describe toluene-d_8 data which are smaller at $c = 0$. To apply the theory of Koyama in the good solvent toluene, it is necessary to assume that the excluded volume effects have negligible influence on the intra particle scattering pattern of the polymer chains. This might be a reasonable assumption in the very low-molecular-weight range $< 10^4$. We therefore tried to modify the parameters l_K and m_L, which occur in the theory of Koyama[7], and used $l_K = 2.9$ nm, $m_L = 460\,g\,nm^{-1}\,mol^{-1}$ and $d = 0.2$ nm, which were estimated from the hydrodynamic radii and the second virial coefficient[8,32]. The maximum heights obtained by this fit are represented as filled squares in *Figure 11*. The values are significantly lower now and in good agreement with the extrapolated ones towards $c = 0$.

Finally, we wish to compare the molecular-weight dependence of the measured global dimensions in toluene with those predicted by equation (16). *Figure 12* represents the result for toluene-d_8, now with the parameters $l_K = 2.9$ nm, $m_L = 460\,g\,nm^{-1}\,mol^{-1}$. Below $M_w = 10^4$ the fit is quite good, which justifies the neglect of excluded volume effects on *intramolecular* scattering behaviour. Above this molecular weight, excluded volume effects become effective.

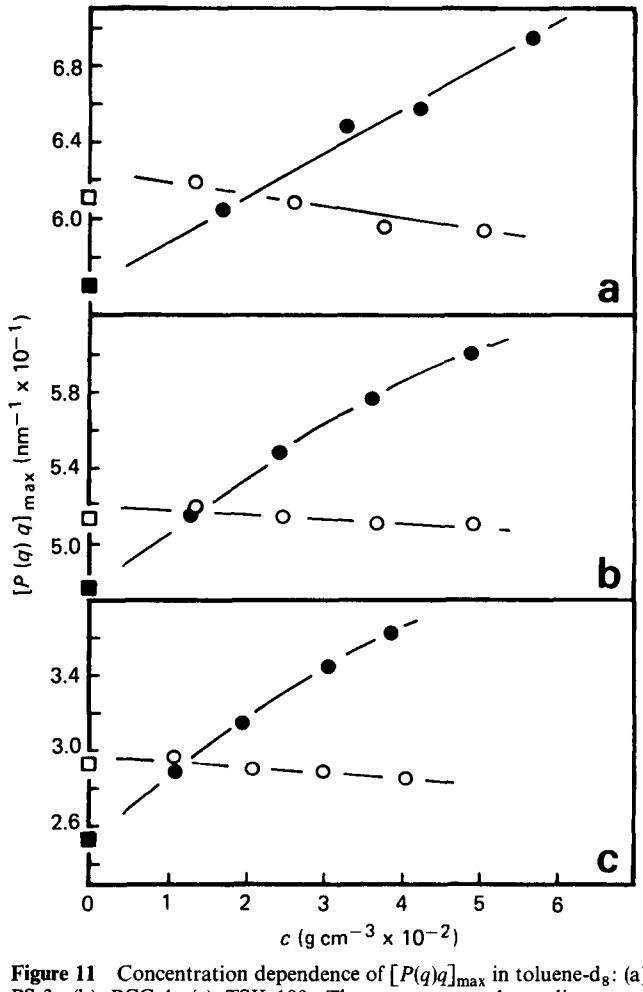

Figure 11 Concentration dependence of $[P(q)q]_{max}$ in toluene-d_8: (a) PS-3, (b) PCC-4, (c) TSK-100. The squares on the ordinate are approximations according to the theory of Koyama[7] where the parameters of *Table 4* were used: (□) PS in cyclohexane, (■) PS in toluene

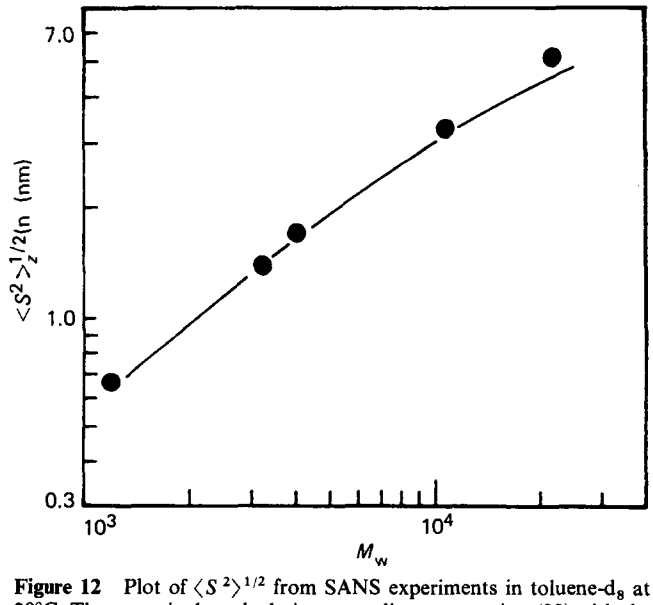

Figure 12 Plot of $\langle S^2 \rangle^{1/2}$ from SANS experiments in toluene-d_8 at 20°C. The curve is the calculation according to equation (22) with the same parameters used to calculate the filled squares in *Figure 11*

THE DENSITY–DENSITY CORRELATION FUNCTION OF ROTATIONAL ISOMERIC STATE CHAINS

As a final point, we would like to discuss the density–density correlation function (CF) $G(r)$:

$$G(r)=\langle\rho(0)\,\rho(r)\rangle \tag{27}$$

This CF is the Fourier transform of the particle scattering factor $P(q)$, given by the following equation:

$$G(r)\sim 1/r\int qP(q)\,\sin(qr)\,\mathrm{d}q \tag{28}$$

In the limit of large objects, there exists an exponential relationship between the number of segments in a sphere and the radius of that sphere, which can be written as

$$R^{D}\sim n_{B} \tag{29}$$

For ordered homogeneous objects $D=d$ is the Euclidean dimension, but for disordered objects, D is less than d and can assume fractional values. Those objects then are called fractals[33]. For Gaussian chains one has $D=2$ and thus with the condition

$$n_{B}=\int_{0}^{R} G(r)4\pi r^{2}\,\mathrm{d}r\sim R^{2} \tag{30}$$

one finds for these chains[39]

$$G(r)\sim 1/r \tag{31}$$

where $G(r)$ is related to $g(r)$:

$$G(r)=n_{B}g(r)/4\pi r^{2} \tag{32}$$

Within the scheme for our Monte Carlo simulations, $G(r)$ can be calculated directly from the probability $g(r)$, which is defined by equation (14). It was of interest now whether the predicted scaling behaviour of equation (31) is already found for the generated short chains.

Figure 13 gives a representation of two CF in logarithmic form, which belong to the particle scattering factors in *Figure 5*. Obviously, chain stiffness decreases the CF in the short r range whereas for large distances the correlation was enhanced. The molecular-weight dependence of $G(r)$ is displayed in *Figure 14* which is complementary to the structure factors of *Figure 6*. The CF of the shortest chain exhibits a strong oscillation in the low r range, which is due to the discrete point

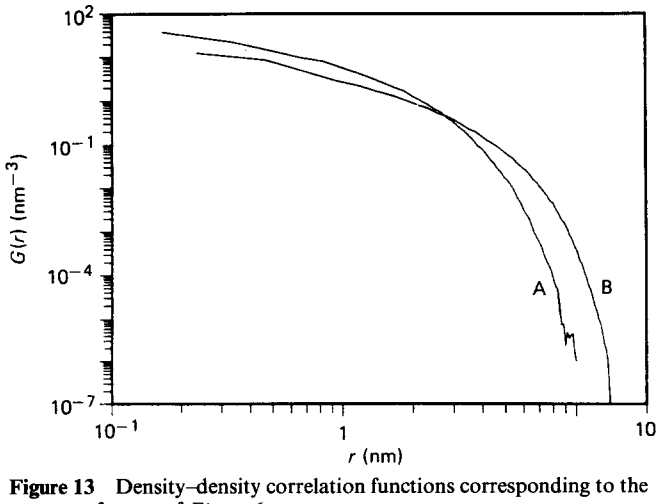

Figure 13 Density–density correlation functions corresponding to the structure factors of *Figure 6*

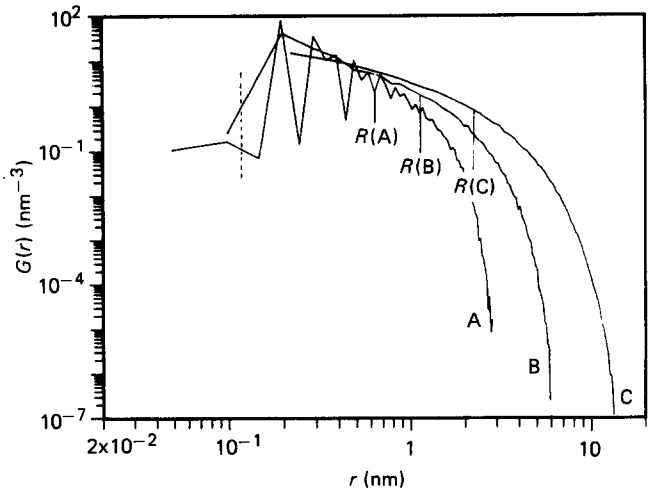

Figure 14 Density–density correlation functions corresponding to the structure factors of *Figure 6*. The broken line indicates the bond length; lines R(A), R(B) and R(C) indicate the corresponding values for $\langle S^{2}\rangle^{1/2}$

character of the backbone chain with fixed distances of next neighbours (0.153 nm). In no case is the scaling behaviour of equation (31), even in an intermediate region, found. Evidently, the chains are much too small to warrant self-similarity, which is an imperative requisite for a fractal. This is in agreement with other calculations[16], which show the fractal behaviour is not obtained before the dimensions ($\langle S^{2}\rangle^{1/2}$) are about 10^3 times larger than the monomeric step length. Our findings are also consistent with the fact that below $n_{B}=205$, an exponential relationship between n_{B} and $\langle S^{2}\rangle$ is not yet found (*Figure 3*).

APPENDIX

Carrying out the sequences of bond transformations onto the C–C backbone bonds and linear combination of the transformed bonds leads to

$$r_{k}=r'_{0}+\sum_{m=1}^{k}\prod_{j=1}^{m}\mathbf{T}_{j}(r'_{m}-r'_{m-1}) \tag{A1}$$

Equation (A1) gives the coordinates of the kth skeletal atom in this conformation[13]. Here $\mathbf{T}_{j}$ is the transformation matrix

$$\mathbf{T}_{j}=\begin{pmatrix}\cos^{2}\alpha_{j}+\cos^{2}\alpha_{j}\sin\chi_{j-1} & \cos\alpha_{j}\sin\alpha_{j}(1-\cos\chi_{j-1}) & -\sin\alpha_{j}\sin\chi_{j-1}\\ \cos\alpha_{j}\sin\alpha_{j}(1-\cos\chi_{j-1}) & \sin^{2}\alpha_{j}+\cos^{2}\alpha_{j}\cos\chi_{j-1} & \cos\alpha_{j}\sin\chi_{j-1}\\ \sin\chi_{j-1}\sin\alpha_{j} & -\sin\chi_{j-1}\cos\alpha_{j} & \cos\chi_{j-1}\end{pmatrix} \tag{A2}$$

attached to the jth bond and $\prod_{j=1}^{m}\mathbf{T}_{j}$ transforms the mth bond from its standard state to the respective state in the final conformation. The angle α_{j} in equation (A2) is defined as

$$\alpha_{j}=\tan^{-1}[(y'_{j}-y'_{j-1})/(x'_{j}-x'_{j-1})] \tag{A3}$$

The prime stands for the standard chain conformation which fixes each bond in the *trans* state. The coordinates (in nm) of the *kth* skeletal bond in the standard chain

conformation are given by:

$$z'_k = 0$$
$$x'_k = k\,0.153\cos((180° - 112°)/2) \qquad \text{(A4)}$$
$$y'_k = \sum_{j=0}^{k} (-1)^{j+1} 0.153 \sin((180° - 112°)/2)$$

ACKNOWLEDGEMENTS

We would like to thank the Institut Max von Laue–Paul Langevin for the use of their neutron scattering facilities. The work was supported by the Deutsche Forschungsgemeinschaft within the scheme of SFB 60.

REFERENCES

1 Flory, P. J. 'Statistical Mechanics of Chain Molecules', Interscience, New York, 1969
2 Kuhn, W. *Kolloid Z.* 1936, **76**, 258; 1939, **87**, 3
3 Kratky, O. and Porod, G. *Rec. Trav. Chim.* 1949, **68**, 1106
4 Ref. 1, Ch. III
5 Ref. 1, pp. 81–5
6 Ref. 1, pp. 147ff
7 Koyama, R. *J. Phys. Soc. Japan* 1973, **34**, 1029
8 Huber, K., Bantle, S., Lutz, P. and Burchard, W. *Macromolecules* 1985, **18**, 1461
9 Institut Max von Laue–Paul Langevin, 'Neutron Beam Facilities Available for Users', Jan. 1981 Edn.
10 Ghosh, R. E., 'A Computing Guide for SANS Experiments at the ILL', 1981, GH 29T
11 Raviseau X., personal communication
12 Kajiwara, K. and Burchard, W. *Macromolecules* 1984, **17**, 2669
13 Hopfinger, A. J., 'Conformational Properties of Macromolecules', Academic Press, New York, 1973
14 Tables of MIT, 1972, collected by G. Sholl
15 Benoit, H. and Doty, P. *J. Chem. Phys.* 1953, **57**, 958
16 Burchard, W., Thurn, A. and Wachenfeld, E., in 'Physics of Finely Divided Matter', Springer Verlag, Berlin, 1985, p. 128
17 Norisuye, T. and Fujita, H. *Polym. J.* 1982, **14**, 143
18 Ballard, D. G. H., Rayner, M. G. and Schelten, J. *Polymer* 1976, **17**, 349
19 Kirkwood, J. G. and Riseman, J. *J. Chem. Phys.* 1948, **16**, 565
20 Vrentas, J. S., Liu, H. T. and Duda, J. C. *J. Polym. Sci., Polym. Phys. Edn.* 1980, **18**, 633
21 Schmidt, M. and Burchard, W. *Macromolecules* 1981, **14**, 210
22 Zierenberg, B., Carpenter, D. K. and Hsieh, J. H. *J. Polym. Sci. Symp.* 1976, **54**, 145
23 Nagai, K. *J. Chem. Phys.* 1963, **38**, 924
24 Debye, P., in 'Light Scattering from Dilute Polymer Solutions', (Eds. D. McIntyre and F. Gormick), Gordon and Breach, New York and London, 1964, p. 139
25 Porod, G. *J. Polym. Sci.* 1953, **10**, 157
26 Holtzer, A. *J. Polym. Sci.* 1955, **17**, 432
27 Neugebauer, T. *Ann. Phys.* 1943, **42**, 509
28 Schmidt, M., Paradossi, G. and Burchard, W. *Makromol. Chem.* 1985, **6**, 767
29 Strazielle, C. and Benoit, H. *Macromolecules* 1975, **8**, 203
30 Witten, T. A. and Sander, C. M. *Phys. Rev. B.* 1983, **27**, 5686
31 Turchin, K. F. 'Slow Neutrons', Israel Program for Scientific Translations, Jerusalem, 1965
32 Huber, K., Burchard, W. and Akcasu, A. Z. *Macromolecules* 1985, **18**, 2743
33 Mandelbrot, B. 'The Fractal Geometry of Nature', W. H. Freeman, New York and San Francisco, 1977
34 The mth moment of a radius is defined as $\langle r^m \rangle = \int W(r) r^m 4\pi r^2 dr$ where $W(r)$ is the radial distance distribution of two chain ends, $m = -1$ gives $\langle 1/r \rangle$